Proton Affinities of Some Amino Acid Side Chains in a Restricted Environment

T. G. Abi, Amit Anand, and Srabani Taraphder*

Department of Chemistry, Indian Institute of Technology, Kharagpur 721302, India

Received: September 29, 2008; Revised Manuscript Received: April 16, 2009

We investigate the dependence of proton affinity values of the side chains of amino acids such as Asp, Glu, His, Ser, and Thr on confinement in a single-walled carbon nanotube. The proton affinity values, estimated using the density functional theories (PW91/dnp and BLYP/dnp), are found to be highly sensitive toward confinement. We find that for both Asp and Glu, the proton affinity, while suspended inside the carbon nanotube, becomes much less in comparison to their respective gas phase values. In the case of His, Ser, and Thr side chains, on the other hand, the proton affinity inside the carbon nanotube becomes negative. Hydrogen bonding with neighboring polar groups is found to result in a marked increase in proton affinity inside the tube in all of the cases reported in this article. The increase is most remarkable in the case of His, Ser, and Thr side chains where the presence of polar neighboring groups within a hydrogen-bonding distance is found to augment the proton affinity value by more than 100 kcal mol^{-1}.

I. Introduction

Proton uptake or release by an amino acid residue in a protein constitutes one of the most commonly encountered processes in bioenzymatic catalyzes.[1] To understand the molecular mechanism of such steps at a given pH, different theoretical and experimental investigations may be designed. For example, to propose the basic mechanistic steps, the protonation states of titrable amino acid residues are often derived based on their pK_a values.[2] However, there may be cases where considerations based on pK_a values alone may not be sufficient to describe the molecular mechanism. In a predominantly nonequilibrium situation, for instance, pK_a measurements give inadequate data about the underlying transition events. Therefore, it may be fundamentally important to investigate the suitability of other reactivity parameters as viable alternatives to be used in such cases.

An interesting yet complicated case study is presented by the isozymes of carbonic anhydrase (CA). In the highly efficient isozyme human carbonic anhydrase (HCA) II, the rate-determining step involves an intramolecular proton transfer between a zinc-bound water (hydroxide) molecule and His-64 (PDB code: 2CBA)[3] with a maximal value of the rate constant $k_B = 800\ ms^{-1}$.[4] This key histidine residue is located in a narrow channel leading from the surface of the enzyme into its active site. It is characterized by a pK_a value of 7.2[4] facilitating proton transfer both from and to His as required by the reversible nature of the catalysis. This residue is also found in the isozymes CA IV and VII at the same location and has been connected to the high catalytic turnovers of these isozymes as well.[5] A much lower efficiency of the isozyme HCA III ($k_B = 3\ ms^{-1}$)[4] has been attributed to the presence of a Lys residue (p$K_a \sim 9$) at the position 64 that is too basic at physiological pH to serve as an efficient proton shuttle.[6] However, mutation of Lys by His (K64H) in HCA III results in a marginal recovery of the catalytic rate with $k_B = 20.0\ ms^{-1}$ in spite of the His residue having a pK_a of 7.5. A somewhat higher efficiency of the proton shuttle may be obtained if a Glu or Asp residue is inserted at the location 64 in HCA III resulting in $k_B \sim 40.0\ ms^{-1}$ where both of the residues exhibit pK_a values equal to 6.4 and 5.7, respectively.[7]

The observed variations in efficiency of the putative proton shuttle as discussed above thus appear to depend not only on the pK_a values but also on various other factors. Rotation of residue 64 through the channel-like pore and a nonequilibrium coupling of the protonation state of the side chain to its fluctuating orientation may be some of the major contributors.[8−11] As already indicated, the presence of specific neighboring residues and internal water molecules may also play a crucial role.[4,8−11] However, the variation of reactivity of different residues such as His, Asp, and Glu at position 64 restricted inside a channel-like environment has not been emphasized so far. In this article, we explore proton affinity (PA) as a reactivity parameter that is not limited by equilibrium considerations and investigate its sensitivity to confinement in a structural pore similar to the ones found in CAs. Interestingly, PA, rather than pK_a, was found to drive the nonequilibrium steps in the photocycle of unidirectional proton transport in bacteriorhodopsin.[12] However, as a prelude to studying the reactivity parameter inside an actual protein, we present in this article the variation of PA in model channel-like pores that closely resemble the one discussed in connection with CAs. We have investigated the proton affinities of some of the polar side chains of amino acid residues only as they are supposed to take part in the proton relay across a protein as suggested by Onsager for a model of long-range biological proton transport.[13,14]

The PA of a molecule is generally defined as the change in enthalpy associated with the addition of a proton to a molecule B in the reaction $B + H^+ \rightarrow BH^+$. This is an extensively studied reactivity parameter of naturally occurring amino acids.[15,16] Conventionally, PA is measured in the gas phase using a wide variety of modern mass spectrometric techniques[17] and kinetic methods.[18] Ab initio and density functional theory (DFT)[19,20] calculations have also been carried out in the gas phase. In general, the PA of a molecule may be estimated as[21]

* To whom correspondence should be addressed. E-mail: srabani@chem.iitkgp.ernet.in.

10.1021/jp808606b CCC: $40.75
Published on Web 06/23/2009

$$\mathrm{PA} = -\Delta E_{\mathrm{el}} - \Delta(\mathrm{ZPVE}) \quad (1)$$

where it is defined as the change in enthalpy as the reactants (B and H^+) are transformed into the product BH^+. In eq 1, $\Delta E_{el} = E(BH^+) - E(B)$ corresponds to the difference in the ground state electronic energies of the protonated and unprotonated forms of the molecule (base) B, respectively. Δ(ZPVE) is the difference in zero point vibrational energies of the protonated and unprotonated forms. It may be noted that at the simplest level, the above equation assumes the PA to be dominated by energetic rather than pressure−volume effects. Additional correction terms to the above expression have also been suggested.[20,22] However, most of these approximate correction terms are rather small as compared to the contributions of the energy changes[20] and would therefore be neglected in our work. Recently, detailed estimates of the PA have been obtained using the Hartree−Fock (HF), second-order Moller−Plesset (MP2), and density functional methods with a range of basis sets.[21,23] It was found that the DFT methods used in conjunction with different basis sets provide accurate PA values within about 1 kcal mol^{-1} of the experimental results[22] in the gas phase.

In this article, we address the calculation of PAs in model systems designed to mimic a chemically inert, restricted environment that closely resembles a channel-like structral pore in a protein structure. In contrast to the reaction shown above, we have considered the protonation reaction as $B + DH^+ \rightarrow BH^+ + D$, where D is a donor of the proton to the base. Because we are interested in computing the PAs in different environments, this representation allows us to take into account the contribution to PA arising from the net enthalpy change of protonation of the base, B, and that of the donor, D. The latter corresponds to the enthalpy of proton hydration if the donor happens to be a water molecule in an aqueous medium.[24−26] In the present work, the base B has been chosen to be the polar side chain of an amino acid residue such as His, Asp, Glu, Ser, or Thr. The donor D is assumed to be a water molecule or an appropriately related group. Different donor−acceptor pairs are thus formed by varying the base B and placed inside the model pore.

In the present work, we have used a single-walled carbon nanotube (CNT) as a model of the desired restricted environment. The CNT has already been studied extensively as a computationally efficient mimic of nonpolar confinement to investigate water filling of nonpolar pores and cavities and transport of several species including water,[27,28] ions,[29] protons,[29−32] nonpolar solutes,[29] peptides, and nucleic acids.[33,34] We have studied here the variation of side chain PA values of the amino acid residues mentioned above when each is present suspended from the wall of the CNT. This has been so designed to simulate, albeit in a highly simplified manner, the location of residue 64 as encountered in CAs. Therefore, only the side chain PA becomes relevant in this set of model studies. It may be noted that the measured PA values in the gas phase (with the noted exception of histidine) correspond to those of the α-amino nitrogen. In this work, for residues other than His, we have used as reference side chain PAs calculated using the density functional theories in the gas phase. We expect to quantify the effect of interactions between the side chain atoms with those constituing the wall of the CNT. The importance of such interactions on the effect of confinement has earlier been demonstrated, for example, by the drying of a water-filled narrow CNT pore[27,35] when the attractive interactions are reduced.

Hydrogen bonding is known to play a crucial role in determining the PA of a molecule in a given environment. In the gas phase, the most stable form of the isolated amino acid molecule is $H_2N-CHR-COOH$. In a solvated structure, where there are 4−5 water molecules in its first solvation shell, the amino acid is stabilized in a zwitterionic ($NH_3^+-CHR-COO^-$) form.[36,37] Hydrogen bonding by the solvent molecules can stabilize the charged states of acidic or basic amino acids in solution[38,39] with the solvent molecules in the first solvation shell contributing significantly to the stability of the charged species. Such stabilization, as expected, increases with the increase in the number of intermolecular hydrogen bonds around the solute molecule.[40] As observed in the case of CAs, the presence of neighboring amino acid residues with hydrogen-bonding centers often promotes the efficiency of a proton shuttle.[8] To mimic this effect, we have also studied model systems where a few polar −OH groups are suspended from the wall of the CNT. As expected, we find that inside the hydrophobic pore, all of the amino acid side chains undergo a significant decrease in PA. However, introduction of hydrogen bonding to some neighboring groups is found to change this scenario drastically. Most interestingly, the side chains of His, Ser, and Thr are found to exhibit a marked increase in PA by 80−130 kcal mol^{-1} when suspended inside the CNT in the presence of hydrogen bonding.

The rest of the article is arranged as follows. We outline the details of our computational method in section II, and the results are presented in section III. Section IV concludes with a brief discussion.

II. Method

In this section, we outline the various computational steps adopted to obtain PAs of a given amino acid inside a CNT. For this purpose, we have studied the following reactions:

$$B + H_3O^+ \rightarrow BH^+ + H_2O \qquad \text{(for gaseous phase)}$$
$$B + -C-OH_2^+ \rightarrow BH^+ + -C-OH \qquad \text{(in CNT)}$$

The PA of the amino acid side chain in a given medium is then calculated as usual being equal to the negative of reaction enthalpy, ΔH, as

$$\mathrm{PA} = -\Delta H = -(\Delta H_1 - \Delta H_2) \quad (2)$$

where ΔH_1 is the difference in enthalpy of the protonated and unprotonated base, while ΔH_2 corresponds to that of the donor (H_3O^+ or $-C-OH_2^+$, as the case may be). In each case, the enthalpy change is estimated as

$$\Delta H_i = \Delta E_i + \Delta \mathrm{ZPVE}_i \; (i = 1, 2) \quad (3)$$

where ΔE_i and $\Delta \mathrm{ZPVE}_i$, as discussed in the Introduction, represent the change in ground state electronic energy and zero point vibrational energy, respectively, on protonation of the base ($i = 1$) or the donor ($i = 2$). We shall next discuss how we construct the model environments and compute the PA in each of them following the method outlined above.

We have first constructed a single-walled, 6:6 armchair CNT of diameter 8.14 Å and length 9.84 Å using the utilities of *Dmol3*.[41] The wall is a lattice composed of sp^2-hybridized C-atoms, while H-atoms are added to both ends of the nanotube. The entire structure is then subjected to geometry optimization using a PWC-LDA functional[42] with minimum basis functions whereby a rapid convergence is obtained. It may be noted that

the CNT of our choice is smaller than those used in earlier studies[27,29−31] to facilitate a fully quantum optimization.

We have subsequently constructed and investigated models having an amino acid side chain suspended from the wall of the CNT for each of the five amino acids under consideration, viz., Asp, Glu, His, Ser, and Thr. The following are the steps adopted in each case. We start by modifying one wall C-atom into a sp^3-hybridized one near the middle of the tube and approximate it as the C_α-atom of a chosen amino acid side chain. The rest of the side chain remains freely suspended inside the core of the tube. The structure thus obtained is optimized using a PWC-LDA functional[42] with minimum basis functions as described above. It may be noted that in these mimics, we do not have the peptide backbone, but we shall still label the suspended segment as the amino acid side chain for the sake of convenience. The same steps were repeated to model the protonated side chain suspended from the wall of CNT. It may be noted that in the case of Asp and Glu side chains, we are essentially looking at the transformation $-COO^- \rightarrow -COOH$. On the other hand, we focus on $=N \rightarrow =NH^+$ for His and $-O^- \rightarrow -OH$ for Ser and Thr side chains.

With the optimized structure (both with and without the excess proton on the side chain), single point energy calculations were carried out using the methods PW91/dnp[43] and BLYP/dnp.[44] In all single point energy calculations, we have used the double numerical polarized (dnp)[45−49] basis sets with diffuse and polarization functions. It is found that both of the methods yield equivalent trends, and so, only the BLYP/dnp method has been used to report the results here. To ensure computational efficiency, a frequency analysis has been carried out considering the partial Hessian matrix of the side chain atoms only.

We have also constructed and studied the model systems where either an $-OH_2^+$ or an $-OH$ group is suspended from the wall of the CNT. The corresponding change in enthalpy, ΔH_2, of protonation of the donor $-OH$ group inside the core of the CNT was estimated following the same steps as discussed above.

While the above model is expected to serve as a mimic of a hydrophobic channel inside a protein, further modifications of the model are necessary to understand the effect of neighboring polar groups inside the tube on the side chain reactivity. For this purpose, we have adopted two more models as described below for each amino acid considered in this work.

In the first polar mimic of the protein channel, we introduce a number of polar $-OH$ groups suspended from the wall by modifying a few more C_α-atoms as described above. These suspended $-OH$ groups are placed within 3.5 Å of the polar side chain atoms so as to be within a hydrogen-bonding distance with them. Let us label this model as HB-CNT. In a second polar model, the polar $-OH$ groups are designed to be located more than 4.5 Å away from the polar atoms of the side chain and will be referred to as the NHB-CNT model. Therefore, the latter model is expected to show the effect of neighboring polar groups, if any, excluding the effect of hydrogen bonding. By replacing the amino acid side chains with $-OH_2^+$ and $-OH$ suspended from the wall, similar model structures were generated with and without hydrogen bonding for the calculation of the corresponding ΔH_2. As before, the geometry optimizations of all of the tube structures were performed using a PWC-LDA method prior to submitting the system for single point energy calculations and estimation of enthalpy changes.

III. Results and Discussion

In this section, we present and discuss the results of our calculations in the model systems outlined above. The optimized structures with the side chains (unprotonated and protonated) extending into the core of the nonpolar tube are shown in Figures 1−5a,b for Asp, Glu, His, Ser, and Thr, respectively. The optimized structures having five $-OH$ groups suspended from the wall along with the amino acid side chain (unprotonated and protonated) within hydrogen-bonding distances have been presented in the panels c and d of these figures. The details of distances between potential hydrogen bond-forming pairs have been highlighted (Figure 6) in the case of unprotonated and protonated side chains of His. In the third model, the structures are similar to those shown in panels c and d of Figures 1−5 with the exception of having the $-OH$ groups located further away from the side chain and have not been shown here. Estimates of enthalpy of protonation of the amino acid side chain, ΔH_1, in the different environments studied are summarized in Table 1. Table 2 shows the variation of enthalpy of protonation of a suitable proton donor, ΔH_2, in different systems. The resultant changes in proton affinities are presented in Table 3.

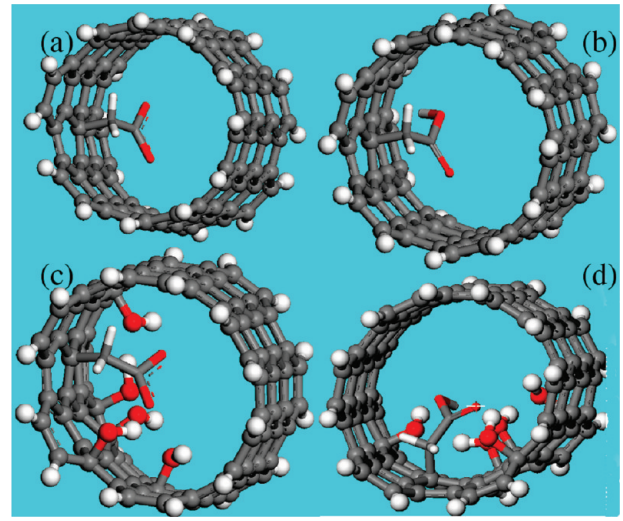

Figure 1. Optimized structures showing the Asp side chain inside a single-walled carbon nantotube suspended from the wall in its (a) unprotonated and (b) protonated forms. Panels c and d show the unprotonated and protonated side chains, respectively, extending into the core of the tube in the presence of five $-OH$ groups suspended from the wall within a distance of 3.5 Å from the side chain atoms.

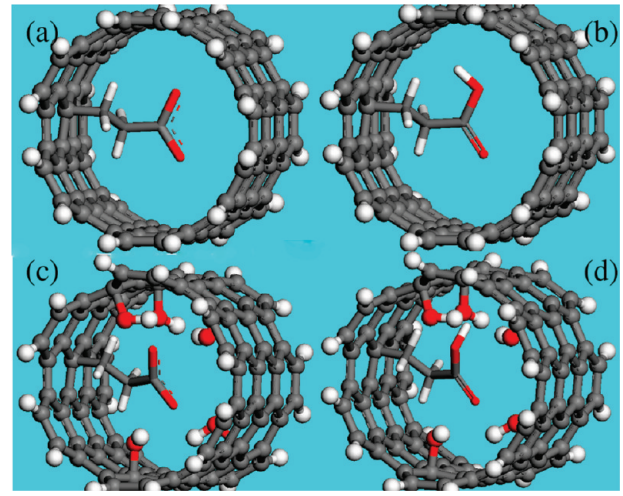

Figure 2. Optimized structures showing the Glu side chain inside a single-walled carbon nantotube suspended from the wall in its unprotonated and protonated forms. Panels a−d correspond to models as described in Figure 1.

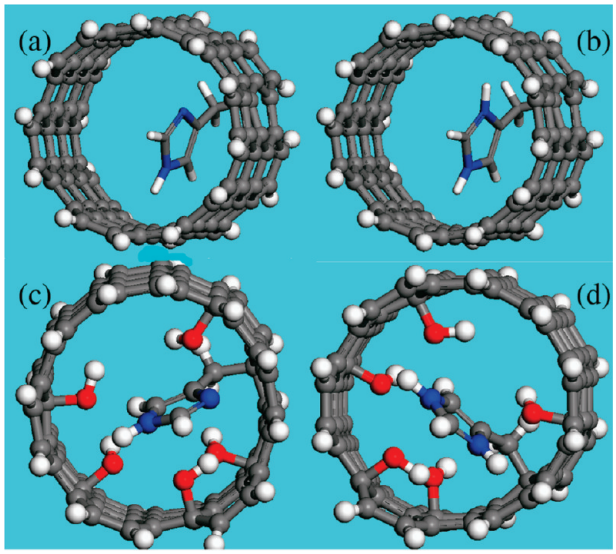

Figure 3. Optimized structures showing the His side chain inside a single-walled carbon nantotube suspended from the wall in its unprotonated and protonated forms. Panels a−d correspond to models as described in Figure 1.

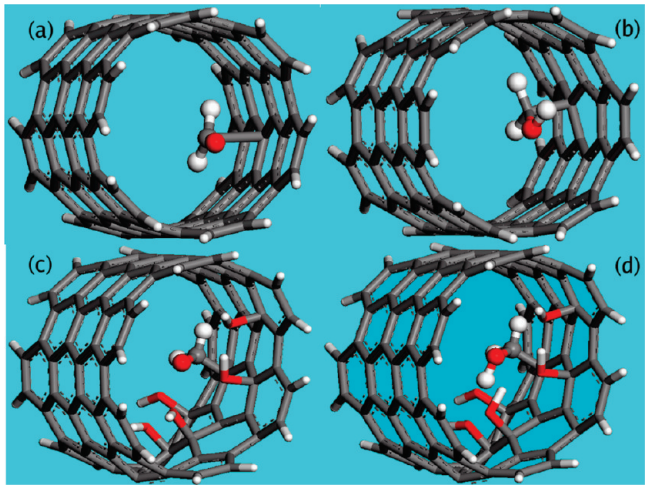

Figure 4. Optimized structures showing the Ser side chain extending into the core of a single-walled carbon nantotube suspended from its wall. The rest of the convention remains the same as in Figures 1−3.

A. Calibration in the Gas Phase. We have first carried out benchmarking studies by computing ΔH_1, ΔH_2, and PA associated with the protonation of a chosen amino acid side chain and a water molecule in the gas phase and comparing them with earlier results, if applicable. Note that ΔH_1 in the gas phase as tabulated in Table 1 actually corresponds to the PA of the base B according to eq 1. The side chain PA of His (equivalently, $-\Delta H_1$) is well-documented in literature. Our estimate of the gas phase PA of histidine side chain equal to 235.11 kcal mol^{-1} is found to correlate well with the experimental values, for example, 231.5[50] and 236.1 kcal mol^{-1}[51] and a theoretical value of 236.4 kcal mol^{-1}[22] reported earlier. It may be noted that our estimates fall well within the maximum reported deviation of DFT-based predictions of PA values in the gas phase.[23] Interestingly, we find that both Ser and Thr exhibit large PAs in the gas phase that exceed those of Asp, Glu, and His. The value of $-\Delta H_1$ of Glu side chain, on account of its additional $-CH_2$ group, is found to be marginally larger than that of Asp, in agreement with earlier observations.[21] The major contribution to the observed behavior appears to have

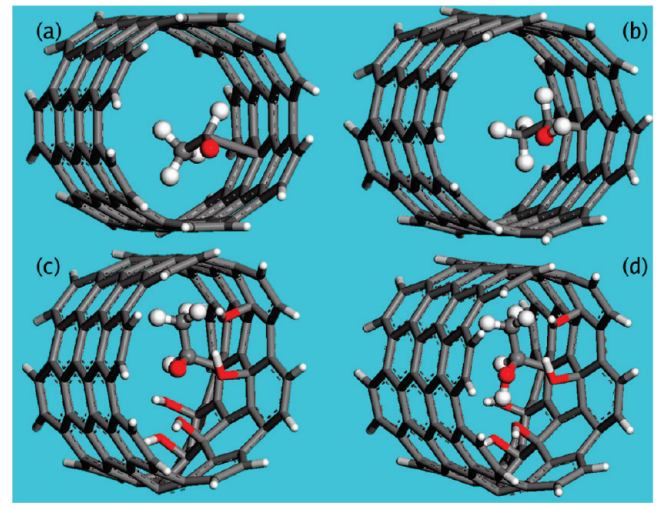

Figure 5. Optimized structures showing the Thr side chain extending into the core of a single-walled carbon nantotube suspended from its wall. The rest of the convention remains the same as in Figures 1−4.

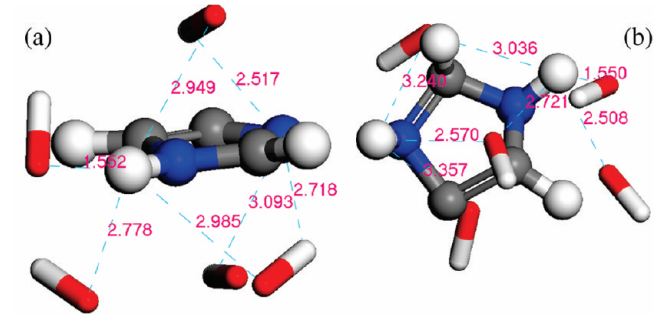

Figure 6. Location of the five −OH groups suspended around the (a) unprotonated and (b) protonated side chains of His inside the CNT. The distances (in Å) between potential hydrogen bond donors and acceptors are shown.

come from the ground state electronic energies as evident from a comparison of ΔH_1 and ΔH_2 values.

B. Enthalpy of Protonation of an Amino Acid Side Chain, ΔH_1, Suspended Inside the CNT. A few key points may be noted from the values of $-\Delta H_1$ shown in Table 1. First, all of the ΔH_1 values are negative irrespective of the amino acid or the model chosen, indicating the protonated form to be more stable than its unprotonated counterpart. A close look at the contributions to ΔH_1 shows that in all of the cases studied here, the change in ΔZPVE on changing the medium is typically less than 15 kcal mol^{-1} and the dominating contribution comes from the change in ground state eletronic energies as we go, for example, from nonpolar CNT to the ones having polar −OH groups suspended in it (HB-CNT and NHB-CNT). Needless to say, there are significant changes in the individual electronic energies as one changes the medium, and these are illustrated in Table 1. To facilitate a direct comparison, we have presented for the CNT models $E_{el} - E_{el}$(tube) by subtracting the ground state electronic energy of the tube itself. Using the BLYP estimates, E_{el}(tube) is found to be equal to 2.3038×10^6 kcal mol^{-1}. It may also be noted that in the HB-CNT and NHB-CNT models, the energy values presented contain not only the donor and the base but also the contribution coming from the five suspended −OH groups.

Let us first investigate the changes in $-\Delta H_1$ in going from the gas phase to the nonpolar CNT. In all of the cases, as expected, the electronic energy increases by transferring the side

TABLE 1: Enthalpy of Protonation, ΔH_1, of Five Amino Acid Side Chains in the Gas Phase and the Three Models of CNT

		kcal mol^{-1}				
system		E(B)	E(BH$^+$)	$-\Delta E$	ΔZPVE	$-\Delta H_1$
gas	Asp	−321177.46	−321528.12	350.66	8.33	342.33
	Glu	−345837.49	−346190.00	352.50	7.92	344.58
	His	−344370.80	−344613.69	242.88	7.77	235.11
	Ser	−250018.33	−250377.88	359.55	8.36	351.19
	Thr	−274670.66	−275042.63	371.97	15.1	356.87
CNT	Asp	−143495.19	−143866.24	371.05	7.10	363.95
	Glu	−168148.37	−168485.68	337.30	6.99	330.31
	His	−166941.42	−167211.12	269.69	7.55	262.14
	Ser	−72444.92	−72735.25	290.33	6.21	284.12
	Thr	−97098.28	−97392.29	294.01	9.91	284.10
NHB-CNT	Asp	−381157.96	−381485.78	327.81	7.10	320.71
	Glu	−405854.60	−406170.03	315.44	6.99	308.45
	His	−404362.03	−404630.42	268.41	7.55	260.86
	Ser	−310087.14	−310371.86	284.69	6.21	278.48
	Thr	−334724.98	−335047.22	322.25	4.55	317.70
HB-CNT	Asp	−381172.35	−381525.62	353.28	7.10	346.18
	Glu	−405792.52	−406153.20	360.69	6.99	353.70
	His	−404233.80	−404630.98	397.16	7.55	389.61
	Ser	−309999.39	−310441.55	442.19	12.03	430.16
	Thr	−334634.20	−335033.56	399.34	1.43	397.91

TABLE 2: Variation of Enthalpy of Protonation of the Donor ΔH_2 Calculated Using the BLYP/dnp Method[a]

	kcal mol^{-1}				
system	E(B)	E(BH$^+$)	$-\Delta E$	ΔZPVE	$-\Delta H_1$
gas	−47968.66	−48142.73	174.07	8.05	166.03
CNT	−48094.43	−48397.43	303.00	6.05	296.95
NHB-CNT	−285762.73	−286069.48	306.75	2.37	304.37
HB-CNT	−285766.358	−286080.05	313.69	5.93	307.76

[a] The donor is assumed to be a protonated water molecule in the gas phase. In the three models of CNTs, the donor is a polar −OH group suspended from the wall of the CNT.

TABLE 3: PA Values of Asp, Glu, His, Ser, and Thr Side Chains in Different Restricted Environments[a]

system		PA (kcal mol^{-1})	system		PA (kcal mol^{-1})
gas	Asp	176.30	NHB-CNT	Asp	16.34
	Glu	178.55		Glu	4.08
	His	69.08		His	−43.51
	Ser	185.16		Ser	−25.89
	Thr	190.84		Thr	13.33
CNT	Asp	67.00	HB-CNT	Asp	38.42
	Glu	33.36		Glu	45.94
	His	−34.81		His	81.85
	Ser	−12.83		Ser	122.40
	Thr	−12.85		Thr	90.15

[a] The values reported in the table have been estimated using the BLYP/dnp method for the calculation of ground state electronic and zero point vibrational energies.

chain (protonated or unprotonated) to the CNT. However, the observed variations in $-\Delta H_1$ for different side chains result directly from a differential destabilization of B and BH$^+$ inside CNT wrt the gas phase. For example, on transferring from the gas phase to the CNT, B is destabilized by about 177680 kcal mol^{-1} for Asp/Glu, 177573 kcal mol^{-1} for Ser/Thr, and 177429 kcal mol^{-1} for His. The corresponding values for the destabilization of BH$^+$ are 177661 kcal mol^{-1} for Asp, 177704 kcal mol^{-1} for Glu, 177650 kcal mol^{-1} for Ser/Thr, and 177402 kcal mol^{-1} for His. It is interesting to note that the protonated Glu side chain undergoes a larger destabilization from its gas phase value, leading to a lower value of $-\Delta H_1$ as compared to that of Asp, consistent with the variations observed in the solution phase.[52] We find that for Glu, Ser, and Thr, $-\Delta H_1$(gas) > $-\Delta H_1$(CNT), while an opposite trend is observed for and Asp and His. For the latter side chains extended into the pore of the nanotube, $-\Delta H_1$ increases by about 21 and 27 kcal mol^{-1}, respectively, as compared to their gas phase values.

In contrast, the variations of $-\Delta H_1$ for the CNT, NHB-CNT, and HB-CNT models are found to be more regular. For all of the side chains except Thr, it is found that the value of $-\Delta H_1$ varies as CNT > NHB-CNT < HB-CNT, while for Thr, the variation is given by CNT < NHB-CNT < HB-CNT. The observed variations are found to result from a subtle interplay of two opposing effects whereby the nonpolar tube prefers the uncharged form of the base, while the polar groups prefer the side chain with an excess charge. In all of the cases studied here, a significant stabilization of the protonated side chains is observed facilitated by the hydrogen-bonding interactions even in the presence of a small number of them. The $-\Delta H_1$ values of Asp and Glu side chains increase by about 25 and 45 kcal mol^{-1} on account of the additional stabilization of the protonated form provided by the hydrogen-bonding interactions. However, the increment is most striking in the case of the His, Ser, and Thr side chains whereby the $-\Delta H_1$ becomes more postitive by about 130, 152, and 80 kcal mol^{-1}, respectively. This clearly shows the extent to which hydrogen bonding to long-lived neighboring groups may promote the stabilization of a protonated side chain inside a predominantly hydrophobic environment.

C. Enthalpy of Protonation of the Donor, ΔH_2, and Overall PA. In Table 2, we present the enthalpies of protonation of a suitable donor in the different model environments that we have discussed so far. It is well-known in literature that the enthalpy of proton hydration depends crucially on the model chosen as well as on the method used.[26,53−55] In our calculations of ΔH_2, we have followed an identical method as that used in the case of protonation of the base B. Our gas phase estimate of the enthalpy of protonation of a water molecule to obtain H_3O^+ (−166.029 kcal mol^{-1}) is close to the experimental value reported earlier (−165.0 kcal mol^{-1}).[54] It is interesting to note that proton solvation by a cluster of eight water molecules was found to give rise to an enthalpy change of −213 kcal mol^{-1}.[54] Using the present method, it is possible to show that $\Delta H_2 = -213.67$ kcal mol^{-1} for the enthalpy of protonation in a water cluster comprised of 14 water molecules in the gas phase. In Table 2, an interesting variation is presented by the case whereby a −OH group in its protonated or unprotonated form is suspended from the walls of the CNT. Once again, the enthalpy of protonation of the donor is dominated by the changes in ground state electronic energies, and a small but significant effect of hydrogen bonding is observed in the presence of polar −OH groups in close proximity.

The overall PAs of the five amino acid side chains are presented in Table 3. To obtain these estimates, we present the results of our calculation using the BLYP/dnp method only, and similar variations predicted by the use of PW91/dnp methods are omitted. With the exception of Thr, it is found that in all other cases, the PA shows the following trend: PA(gas) ≫ PA(CNT) > PA(NHB-CNT) ≪ PA(HB-CNT). In the case of Thr, because of the anomalous stabilization of its protonated form in the model, NHB-CNT, the variation turns out to be PA(gas) ≫ PA(CNT) < PA(NHB-CNT) ≪ PA(HB-CNT). The PA of the Glu side chain remains marginally higher than that of Asp in the gas phase as well as in the hydrogen-bonded model HB-CNT. As shown in Table 3, the side chains of His, Ser, or Thr would not prefer to accept a proton inside a nonpolar CNT

on account of a negative value of PA. On the other hand, introduction of the hydrogen-bonding interaction with neighboring polar groups is found to increase the PA of these side chains to such an extent that they become comparable to their respective values in the gas phase. The trend observed for these side chains presents an interesting competition between the enthalpies of protonation of the base and the donor. Inside the CNT, although the existence of the protonated side chain is associated with a large increase in $-\Delta H_1$, the unfavorable contribution from $-\Delta H_2$ inside the tube more than offsets it, leading to the observed negative PA value. Hydrogen bonding therefore becomes all the more important whereby a greater degree of stabilization in terms of ΔH_1 is achieved and makes up for the unfavorable enthalpy changes associated with the (de)protonation of the suspended −OH group inside the CNT.

IV. Conclusion

In this work, we have reported the results of our calculations on the effects of confinement and hydrogen bonding on a crucial reactivity parameter such as PA. We find that in comparison to the gas phase, the PA values may vary widely if the amino acid side chains are present within a restricted environment such as a single-walled CNT. The dimension of the latter was chosen so as to accommodate the side chains of five different amino acids. The largest distance between the C_α atom to the end atom of the side chain is found in the case of protonated His in the model HB-CNT equal to 6.1 Å that is smaller than the diameter of 8.14 Å of the CNT. Hydrogen bonding is found to play a crucial role in promoting the PA value of the side chains. This leads to a remarkable increase in the PA value of His, Ser, and Thr side chains when they are present suspended inside a CNT and hydrogen bonded to neighboring polar groups. Such enhanced PA corroborates well with the fact that some of these amino acid residues are often found in proteins located at narrow channels through which proton transfer pathways pass.

It may be noted that the results presented here, unlike the earlier simulations of water transport in CNTs,[29] assume a model of an isolated CNT in the gas phase. This of course is a highly idealized situation that may be sufficient to take into account PA variations in a hydrophobic pore with little or no contribution of local polarity. In addition, the absence of any solvent makes this description applicable only as a baseline estimate. However, this simplification was retained in our model by choice. This is because we aimed at obtaining an estimate of the sensitivity of PA to confinement free from any complication such as a dynamical water wire extending into the pore or fluctuations of the side chain orientations. In principle, one may study the PA of a free amino acid residue confined inside the channel. However, that would involve considerations of the effect of the residue diffusing through the channel. In addition, such a model would be unsuitable to study the systems such as CAs where the key residue and other stabilizing groups are indeed present suspended from the wall of the structural pore. Moreover, computational efficiency of a fully quantum optimization of the various structural models needed to be taken into account. Thus, the models presented here are expected to serve as reference systems for the calibration of reactivity parameters such as PA in a more realistic situation. The results presented in this article explain qualitatively why insertion of His, Glu, or Asp may account for the recovery of catalytic activity in HCA III. In the light of the PA values of Thr and Ser reported here, it will be interesting to design new experimental studies whereby Lys-64 is mutated with either of these two residues and investigate if a higher catalytic efficiency is observed. However, it is still too premature to try and obtain a quantitative correlation including other factors as mentioned above. Work is in progress in this direction.

In this article, we have presented the proton affinities of all of the amino acids having charged side chains except for Lys and Arg. On account of their much longer side chains, it was not possible to fit them into the model CNT that we have described here. It may be pointed out here that all of the optimized structures presented here are characterized by small yet nontrivial changes in charge distribution at the atom centers (including those constituting the wall of CNT) with the change in protonation state of the suspended side chain. These variations significantly affect the observed changes in PA, making the analysis quite challenging. Any changes in the dimension of the CNT would further complicate the situation and were avoided in this work. At the simplest level, one may try to model these long side chains with a truncated one where, for example, the amine group would be linked directly to the C_α-atom. Our estimates using the method described in this article show that neither Lys nor Arg would exhibit positive PA even in the model HB-CNT. However, as seen from the variations in Asp and Glu, the presence of $-CH_2$ groups may significantly alter these values.

Another promising direction for the improvement of the present models would be to include the backbone of the amino acid in the walls of the CNT. However, this requires a major structural modification of the CNT that poses serious challenges to a geometry optimization using the LDA functionals as reported in the present study. As an alternative approach to probe the effects of the backbone on the PA values, we have generated for histidine an optimized structure whereby in addition to the side chain, $-NH_2$ and −COOH groups are linked to the C_α-atom and extend into the pore of the CNT. The C_α-atom served as the point of suspension from the wall as before. In this model, however, optimization of the structure with a protonated side chain was found to be difficult for more than two −OH groups within the hydrogen-bonding distance. It is also found that the observed PA values depend crucially on the location and number of −OH groups present as the latter can participate in hydrogen bonding with the backbone also. For example, our preliminary calculations using PW91/dnp method show the following result in the presence of two polar −OH groups suspended from the wall within hydrogen-bonding distance. The $-\Delta H_1$ values are found to to be 232.19 and 191.87 kcal mol^{-1}, respectively, with and without backbone atoms, thereby indicating an increase by about 40 kcal mol^{-1} in the $-\Delta H_1$ values. However, the structural changes induced to accommodate both the −OH groups as well as the backbones are quite significant and make a direct comparison with the values reported here untenable. We hope to address these issues in greater detail in future.

Acknowledgment. We sincerely thank Prof. P. K. Chattaraj and Prof. T. Pathak for several helpful comments and discussions. This study was supported in part by a grant from the Council for Scientific and Industrial Research (CSIR), India.

Supporting Information Available: Estimation of proton affinities of amino acid side chains in finite water clusters. This material is available free of charge via the Internet at http://pubs.acs.org.

References and Notes

(1) Hynes, J. T.; Klinman, J. P.; Limbach, H.; Schowen, R. L. *Hydrogen Transfer Reactions*; John-Wiley: New York, 2007.
(2) Gerencser, L.; Maroti, P. *Biochemistry* **2001**, *40*, 1850.

(3) Häkansson, K.; Carlsson, M.; Svensson, A.; Liljas, A. *J. Mol. Biol.* **1992**, *227*, 1192.
(4) Elder, I.; Fisher, Z.; Laipis, P. J.; Tu, C.; McKenna, R.; Silverman, D. N. *Proteins: Struct. Funct. Bioinf.* **2007**, *68*, 337.
(5) Qain, M.; Earnhardt, J. N.; Wadhwa, N. R.; Tu, C.; Silverman, D. N. *Biochim. Biophys. Acta* **1999**, *1434*, 1.
(6) Silverman, D. N.; Tu, C.; Chen, X.; Tanhauser, S. M.; Kresge, A. J.; Laipis, P. J. *Biochemistry* **1993**, *32*, 10757.
(7) Qain, M.; Tu, C.; Earnhardt, J. N.; Laipis, P. J.; Silverman, D. N. *Biochemistry* **1997**, *36*, 15758.
(8) Silverman, D. N. *Biochim. Biophys. Acta* **2000**, *1458*, 88.
(9) Voth, G. A. *Acc. Chem. Res.* **2006**, *39*, 143.
(10) Roy, A.; Taraphder, S. *J. Phy. Chem. B* **2007**, *111*, 10563.
(11) Roy, A.; Taraphder, S. *J. Phys. Chem. B* **2008**, *112*, 13597.
(12) Onufriev, A.; Smondyrev, A.; Bashford, D. *J. Mol. Biol.* **2003**, *332*, 227.
(13) Onsager, L. In *The Neurosciences*; Quarton, G., Melnechuk, T., Schmitt, F. O., Eds.; Rockefeller University Press: New York, 1967; pp 75−79.
(14) Onsager, L. *Science* **1969**, *166*, 1359–1364.
(15) Harrison, A. *Mass Spectrom. Rev.* **1997**, *16*, 201.
(16) Martrenchard-Barra, S.; Dedonder-Lardeux, C.; Jouvet, C.; Solgadi, D.; Vervloet, M.; Gregoire, G.; Dimicoli, I. *Chem. Phys.* **1999**, *16*, 201.
(17) Bojesen, G. *J. Am. Chem. Soc.* **1987**, *109*, 5557.
(18) Mirza, S. P.; Prabhakar, S.; Vairamani, M. *Rapid Commun. Mass Spectrom.* **2001**, *15*, 957.
(19) Wolfram, K.; Holthausen, M. C. *A Chemist Guide to Density Functional Theory*; John-Wiley: New York, 2001.
(20) Rao, J. S.; Sastry, G. N. *Int. J. Quantum Chem.* **2006**, *106*, 1217.
(21) Maksic, Z. B.; Kovacevic, B. *Chem. Phys. Lett.* **1999**, *307*, 497.
(22) Dinadayalane, T. C.; Sastry, G. N.; Leszuczynski, J. *Int. J. Quantum Chem.* **2006**, *106*, 2920.
(23) Smith, B. J.; Radom, L. *Chem. Phys. Lett.* **1994**, *231*, 345.
(24) Donald, H. A.; Hugh, M. W.; Davidson, W. R.; Pogban, T.; Hopkins, H. P.; Moulik, S. P.; Jahagirdart, D. V. *J. Am. Chem. Soc.* **1991**, *113*, 1770.
(25) Swart, M.; Rosler, E.; Bickelhaupt, M. *Eur. J. Inorg. Chem.* **2007**, *2007*, 3646.
(26) Mejias, J. A.; Hugh, M. W.; Lago, S. *J. Chem. Phys.* **2000**, *113*, 7306.
(27) Hummer, G.; Rasaiah, J. C.; Noworyta, J. P. *Nature* **2001**, *414*, 188.
(28) Berezhkovskii, A.; Hummer, G. *Phys. Rev. Lett.* **2002**, *89*, 6.
(29) Rasaiah, C.; Garde, S.; Hummer, G. *Annu. Rev. Phys. Chem.* **2008**, *59*, 713.
(30) Burykin, A.; Warshel, A. *J. Comput. Theor. Nanosci.* **2006**, *3*, 237.
(31) Hassan, S. A.; Hummer, G.; Lee, Y. S. *J. Chem. Phys.* **2006**, *124*, 204510.
(32) Zhu, F.; Schulten, K. *Biophys. J.* **2003**, *85*, 236.
(33) Yeh, I.; Hummer, G. *Proc. Natl. Acad. Sci. U.S.A.* **2004**, *101*, 12177.
(34) Chun Ke, P.; Qiao, R. *J. Phys.: Condens. Matter* **2007**, *19*, 373101.
(35) Waghe, A.; Rasaiah, J. C.; Hummer, G. *J. Chem. Phys.* **2002**, *117*, 10789.
(36) Shoujun, X.; Nilles, J. M.; Bowen, K. H., Jr. *J. Chem. Phys.* **2003**, *119*, 10696.
(37) Lemoff, A. S.; Bush, M. F.; Williams, E. R. *J. Am. Chem. Soc.* **2003**, *125*, 13576.
(38) Fulscher, M. P.; Mehler, E. L. *Chem. Phys.* **1996**, *204*, 403.
(39) Steiner, T. *Biophys. Chem.* **2002**, *95*, 195.
(40) Meotner, M. *Int. J. Mass Spectrom.* **2003**, *227*, 525.
(41) Delley, B. *Comput. Mater. Sci.* **2000**, *17*, 122.
(42) Wu, X.; Gao, Y.; Zeng, X. C. *J. Phys. Chem. C* **2008**, *112*, 8458.
(43) Perdew, J. P.; Wang, Y. *Phys. Rev. B* **1992**, *45*, 13244.
(44) Becke, A. D. *Phys. Rev. A* **1988**, *88*, 3098.
(45) Williams, S. D.; Edwards, E. E. *Int. J. Mol. Sci.* **2004**, *5*, 67.
(46) Lee, S. U.; Han, Y. K. *J. Mol. Struct. (Theochem)* **2004**, *672*, 231.
(47) Delley, B. *J. Chem. Phys.* **1990**, *92*, 508.
(48) Delley, B. *J. Phys. Chem.* **1996**, *100*, 6107.
(49) Delley, B. *Int. J. Quantum Chem.* **1998**, *69*, 423.
(50) Li, X.; Harrison, A. G. *Org. Mass Spect.* **1993**, *28*, 366.
(51) Hunter, E. P. L.; Lias, S. G. *J. Phys. Chem. Ref. Data* **1998**, *27*, 413.
(52) Wolf, J. F.; Staley, R. H.; Koppel, I.; Taagepera, M.; McIver, R. T., Jr.; Beauchamp, J. L.; Taft, R. W. *J. Am. Chem. Soc.* **1977**, *99*, 5417.
(53) Marcus, Y. *Ion Solvation*; John-Wiley: New York, 1985.
(54) Kebarle, P.; Searles, S. K.; Zolla, A.; Scarborough, J.; Arshadi, M. *J. Am. Chem. Soc.* **1967**, *89*, 6393.
(55) Zolotoy, N. B. *Doklady Phys. Chem.* **2006**, *406*, 30.

JP808606B